

1 **Damage propagation rate and mechanical properties of recycled steel fiber-**
2 **reinforced and cement-bound granular materials used in pavement structure**

3

4 **Ahmed Hilal Farhan^{1,*}, Andrew Robert Dawson², Nicholas Howard Thom²**

5 ¹Department of Civil Engineering, College of Engineering, University of Anbar, Anbar, Iraq

6 Tel: +964 7805521276, E-mail: ahmed.farhan_ce@uoanbar.edu.iq, ahmed.farhan2010@yahoo.com

7 ²School of Civil Engineering, Faculty of Engineering, University of Nottingham, University Park,

8 Nottingham, NG7 2RD, UK,

9 *Corresponding author.

10

11 **Abstract**

12 Cement-bound granular mixtures (CBGMs) represent an attractive option to increase load-
13 carrying capacity and sustainability in highway construction. However, reflection cracking of
14 overlying pavement layers due to the low tensile strength of CBGMs represents an important
15 obstacle limiting their use. This study is undertaken to investigate how incorporation, in
16 CBGMs, of recycled steel fibers extracted from old tires, at different cement levels may affect
17 their tensile properties related to pavement design. A combination of three levels of cement
18 (3%, 5% and 7% by wt. of aggregate and fiber) and two reinforcement contents (0% and 0.5 by
19 volume of aggregate) was investigated. To comprehensively quantify the benefits of fibers in
20 the presence of variable cement contents, time-dependent fracture and damage propagation
21 were examined quantitatively utilizing a combination of macro-surface cracks, fractal analysis
22 and both image monitoring and processing techniques. The results indicated better tensile
23 strength and toughness after cement and fiber inclusion. Furthermore, increasing the amount of
24 cement accelerates the crack propagation and damage dispersion rate while these two
25 parameters reduced significantly in the case of fiber-reinforced cemented aggregate. All
26 benefits gained from fiber usage are more evident at higher cement contents.

27 **Keywords:** fiber-reinforced cement-stabilized mixture; recycled steel fibers; tensile testing;
28 fractal analysis; crack propagation speed; damage propagation rate

29
30

31 **1. Background**

32 Cement stabilized aggregate mixture is a cementitious material that consists of aggregate,
33 cement and a small amount of water. Over the years, researchers have attempted to use other
34 stabilizers such as lime (Mohammadinia et al. 2017), flyash (Mohammadinia et al. 2017), kiln
35 dust (Arulrajah et al. 2017) and geopolymers (Arulrajah et al. 2016). To save natural resources
36 and to encourage sustainable solutions, many investigations have been conducted to replace the
37 natural aggregate by recycled aggregate such as recycled concrete aggregate RAC (Li et al.
38 2010) and recycled asphalt pavement RAP (Taha et al. 2002, Puppala et al. 2017) or including
39 waste aggregate such as a mix of construction and demolition waste CDW (Xuan et al. 2012)
40 and glass materials (Arulrajah et al. 2015).

41

42 Cement stabilization of granular materials, intended to be used as a main structural layer within
43 semi-rigid pavements, has been proved as an effective technique giving better protection of
44 weak subgrades and enhanced support for the surface hot mix asphalt layer. However, the
45 inherent crack susceptibility of this layer, either due to shrinkage or due to low tensile capacity,
46 might forms an obstacle that reduces the benefits of the technique. The crack networks that
47 develop normally affect these stabilized layers detrimentally since they reduce the structural
48 integrity, contributing negatively to load-carrying capacity, and most importantly increase the
49 possibility of reflection cracking, especially in the case of wide cracks.

50

51 Many attempts have been made to overcome the disadvantages that accompany application of
52 cement stabilization in pavement construction. Thompson (2001), Shahid (1997) and Coni and
53 Pani (2007), for example, tried to use industrial steel fibers as a reinforcement and investigated
54 how such reinforcement might affect the mechanical properties of cement-stabilized aggregate

55 mixtures. Their results indicated the better mechanical behavior of the composite. Different
56 types of fiber have also been used in many applications to improve the properties of different
57 types of chemically stabilized soils (Mirzababaei et al. 2012, Chen et al. 2015, Balkis 2017,
58 Cristelo et al. 2017) . Coni and Pani (2007) claimed that the initial cost of this industrial fiber
59 might make it an uneconomic option while Sobhan and Mashnad (2002) and Sobhan and
60 Mashnad (2003) justified their design in the light of other benefits such as longer fatigue life
61 and reduced layer thickness. Nevertheless, they later attempted to use the waste fibers extracted
62 from old milk containers to reduce the initial cost of the fibers and hence reduce the pavement
63 construction cost while ensuring better performance and a sustainable pavement structure. In
64 their study, Zhang et al. (2013) used polypropylene fibers as a low price reinforcement in
65 CBGMs. Improvement in fracture properties was the main outcome of their investigation.
66 More recently, Farhan et al. (2015) and Farhan et al. (2016) used rubber particles from recycled
67 vehicle tires as replacement for fine aggregate to modify the aggregate mixture and hence
68 ensure better mechanical and cracking behavior. These rubber particles, as their results
69 indicated, affect many of the mechanical properties detrimentally but achieve better cracking
70 characteristics.

71

72 In order to improve mechanical properties while ensuring reduced cost and maintaining a
73 sustainable pavement structure, an attempt is made in this paper to use recycled steel fibers
74 from old tires as a reinforcement. Despite the recent use of this recycled reinforcement in
75 different types of concrete as reported in many investigations (Aiello et al. 2009,
76 Angelakopoulos et al. 2015, Caggiano et al. 2015), the use of recycled steel fibers has never
77 been attempted in cement-stabilized aggregate at relatively low cement contents.

78

79 Investigation of damage propagation and cracking patterns is of the utmost importance since it
80 will help in the understanding of damage and hence failure mechanisms which will eventually
81 lead to more optimized mixtures (Silva et al. 2009). For concrete mixtures used in different

82 civil engineering structures, many studies have been conducted to examine the crack
83 propagation speed in both plain and fiber-reinforced concretes. Mindess (1995) conducted a
84 study to show how fiber inclusion in normal concrete mixtures affects the crack propagation
85 speed. He reported a decline in crack speed after steel fiber inclusion. Pyo et al. (2016) noted
86 that the number of studies to characterize crack propagation in fiber-reinforced concrete is very
87 limited compared to those performed for plain concrete and, accordingly, they studied the effect
88 of fiber and loading rate on crack propagation speed in ultra-high strength concrete. Their
89 findings indicated a drop in the crack propagation speed due to fiber reinforcement.

90

91 To the best knowledge of the authors, all of the above-mentioned studies to investigate the
92 impact of fibers (either industrial or recycled) have focused on the mechanical properties only
93 and no study has so far been conducted to investigate crack propagation in either plain or fiber-
94 reinforced cement-stabilized mixtures. Furthermore, the role that cement content might play in
95 this process is still unclear. Therefore, this study has been undertaken to investigate how fiber
96 inclusion at various cementation levels might affect the mechanical properties and to
97 understand the effect of fiber inclusion on the crack propagation process in cemented aggregate,
98 as a time-dependent phenomenon.

99

100 **2. Experimental methodology**

101 **2.1 Materials**

102 A limestone aggregate from Tunstead Quarry, Derbyshire, UK was used in this study. The
103 gradation is shown in Figure 1 together with specification limits.

104

105 To reduce the cost and increase the sustainability of highway pavement construction, recycled
106 steel fibers (Figure 2) were incorporated to reinforced cement-stabilized aggregate mixtures.
107 These were extracted from old vehicle tires by a shredding process. The maximum fiber
108 volumetric content attempted in cement-bound granular materials (CBGMs) is 1% as

109 documented in previous literature (Shahid 1997, Thompson 2001). Trial investigations at the
110 start of the current experimental program showed there was difficulty in achieving uniform
111 fiber dispersion due to fibers balling at 1% volumetric content. To ensure uniformity of fiber
112 dispersion, a 0.5% volumetric content was selected.

113

114 Portland cement (CEM I 52.5 N) was used for the purpose of stabilization and binding the
115 mixture components. To examine the effect of stabilizer content on the performance and
116 effectiveness of fibers in CBGMs, three different stabilization levels, 3%, 5% and 7% by dry
117 weight of aggregate and fibers were used. These cement contents, together with design water
118 contents, were chosen based on the results of a previous investigation (Farhan et al. 2016).

119

120 **2.2 Mix design**

121 First, aggregate fractions were combined to produce CBGM 2-0 (BS EN 14227-1:2013 (British
122 Standards Institution 2013)). To avoid any variability in aggregate gradation, each specimen
123 was batched, mixed and compacted individually.

124

125 In this paper, a combinations of two fiber contents (0 and 0.5% by weight of dry aggregate) and
126 three cement contents (3%, 5% and 7% by weight of dry aggregate plus fibers) were evaluated.

127 For these fiber-reinforced CBGMs mixtures (i.e. FCBGMs), water contents were proportioned
128 by the weight of dry aggregate, cement and fibers. Although a volumetric basis should be
129 logically used to determine the required amount of water, using weight proportions resulted in
130 negligible error due to the small amount of fibers used. Table 1 shows the investigated mixture
131 designations and proportions.

132

133 **2.3 Mixing, manufacturing and curing**

134 The aggregate was mixed first with cement for a minute. Then, the design water content was
135 added and mixed for two minutes. Lastly, the steel fibers were added and mixed for another one
136 minute with the wet cemented aggregate. The mixing process was conducted manually.

137 The fresh cemented aggregate-fiber mixture was compacted in lubricated steel molds using a
138 Kango 638 vibratory hammer. All compacted specimens were kept molded for the rest of the
139 day then demolded, wrapped, and stored in wet plastic bags for 28 days. After the curing period,
140 specimens were trimmed to obtain 100 mm x 100 mm cylindrical samples. As can be observed
141 in Figure 3a, even for lower cement content, specimens looked intact and no pulling out of
142 fibers was noticed, which suggests good interaction and bonding with aggregates.

143

144 **2.4 Indirect tensile testing setup**

145 CBGMs are normally classified through system II of European standards BS EN 14227-1:2013
146 based on their tensile strength. Adopting tensile strength comes from the fact that all
147 cementitious stabilized layers within semi-rigid pavement structures are designed to resist the
148 tensile stresses generated at lower boundary. Therefore, in this paper, tensile properties were
149 utilized to evaluate the investigated mixtures. Indirect tensile testing was conducted on
150 specimens at 28 days using a UTM-Instron with 200 kN capacity by applying a diametrical
151 compression on the specimen. The application of this load was achieved through a curved steel
152 plate. The latter step was preceded by marking of the specimen center to avoid eccentricity of
153 loading. Indirect tensile strength (ITS) was calculated as $ITS = \frac{2P}{\pi hd}$, where P= Peak load, N;
154 h= specimen thickness, mm and D= specimen diameter, mm. Density was measured using the
155 water-displacement method.

156

157 **2.4.1 Stress- strain curves, absolute toughness and ductility**

158 During vertical load application, horizontal strains were captured using non-contact equipment.
159 This system is a video-based 2D measuring tool, called “Video Gauge”, for observing a face of
160 a specimen under test. It consists of a lighting source and a high-resolution camera. The
161 measurement is conducted by employing a digital image correlation (DIC) algorithm provided
162 in the accompanying software. Figures 3b & 3c illustrate the testing setup and instrumentation
163 system used in this investigation. Specimen faces were first speckled by application of a thin

164 white matt paint followed by a thin black paint as shown in Figure 3a, c. The test was performed
165 at a rate of 0.5 mm/min.

166

167 The load-carrying capacity or material toughness was calculated as the area under the stress-
168 strain (Shahid 1997). For all investigated mixtures, this area was calculated up to strain of 2.5%.
169 This approach evaluates the effect of both ductility and strength on material toughness due to
170 steel fibers inclusion (Sobhan and Mashnad 2000). The formula due to Park (2011) was used
171 to evaluate material ductility in terms of deformability index (Di) which can be calculated as,
172 $D_i = \Delta_{fibrous} / \Delta_{nonfibrous}$, where $\Delta_{fibrous}$ and $\Delta_{nonfibrous}$ are the horizontal strains at peak
173 stresses of fibrous and non-fibrous specimens, respectively.

174

175 **3. Results and explanations**

176 **3.1 Combined effect of cement and fibers on indirect tensile strength and density**

177 In general, the observed trend (Figure 4) is that the ITS value increases as cement content
178 increases for both CBGMs and FCBGMs. This is logical in the light of the improvement
179 occurring in the bond between aggregate particles with increase of cement content which, in
180 turn, increases hydration products after curing. This will ensure, at the same time, better bond
181 with fibers which increases the tensile strength. This is because the fibers inside the specimen
182 will carry part of the load and also might prevent crack propagation and hence ensure intactness
183 of the specimen. For this reason, the improvement in ITS value after fiber incorporation seems,
184 as shown in Figure 4, most obvious at higher cement content. The inclusion of fibers at 3%
185 cement content does not have any effect on ITS whereas the percentage improvement in ITS
186 value is 16% and 40% due to fiber incorporation at 5% and 7% cement content, respectively.

187

188 Except for lightly cemented mixtures, densities rose after fiber reinforcement as presented in
189 Table 1. This is because the specific gravity of the added fibers is much higher than the natural
190 limestone aggregates.

191 **3.2 Combined effect of cement and fiber on stress-strain curves and toughness**

192 The stress-strain relationships for the mixtures investigated are shown in Figure 5. In all
193 CBGMs with different cement contents, strain-softening occurs following initial cracking
194 whereas this is not the case for fiber-reinforced mixtures. FCBGMs showed a strain-hardening
195 zone after first crack initiation enabling them to carry an additional tensile load before reaching
196 their ultimate capacity. The presence of enough cement ($\geq 5\%$) allows the reinforcement system
197 to carry the applied tensile stress after yielding of the cemented aggregate. After reaching their
198 ultimate strength, all mixtures at all cement and fiber contents showed strain-softening.
199 However, the degree of softening differed depending on cementation and reinforcement levels.

200

201 In terms of toughness improvement (Figure 6), the more the cement content the better the
202 toughness of both reinforced and unreinforced mixtures. Furthermore, toughness improvement
203 after reinforcement depends, to a large extent, on the cement content. In heavily cemented
204 mixtures, fiber addition improves toughness significantly compared to lightly cemented
205 mixtures; increases of 129%, 247% and 429% after 0.5% fiber incorporation are seen at cement
206 contents of 3%, 5% and 7%, respectively. This might be attributable to a lower rate of crack
207 propagation because the presence of fibers arrests the cracks and the degree to which crack
208 propagation is inhibited is largely governed by the bond strength (i.e., the amount of cement)
209 between the fibers and surrounding materials.

210

211 **3.3 Combined effect of cement and fibers on ductility**

212 Strain at peak stress generally decreases in CBGMs as the amount of cement increases as shown
213 in Figure 7. This is because, as is well-known, the addition of more cement increases the
214 brittleness of the mixture which may lead to failure with little deformation. In contrast, after
215 0.5% fiber reinforcement, the strain at peak increases substantially. This improvement, as was
216 obtained from other findings, also seems to be governed by the cement content. Consequently,
217 the trend of deformation index, due to fiber inclusion, is for significant improvement as cement

218 content increases, with a deformability index increase of 16 and 11 times after fiber addition at
219 cement contents of 5% and 7%, respectively compared with that at 3%. It seems that the
220 presence of fibers in a highly cemented “environment” causes an increased restraint which in
221 turn reduces the deformation of the specimens. This may explain the reduced deformability of
222 fiber-reinforced mixtures at 7% cement content compared to 5%. Enhancement in ductility due
223 to fiber reinforcement was also reported by Kim et al. (2010), who studied the effect of fibers
224 on ductility of concrete. The effect of restraint was also noticed in their investigation where the
225 largest reported ductility was at a lower fiber content, 0.25%.

226

227 **4 Time-dependent fracture damage propagation**

228 One of the most important problems, representing a serious challenge to the application of
229 cement-bound granular mixtures is their sensitivity to cracking, either from bottom-up fatigue
230 or from shrinkage. If they are wide, these cracks contribute to a reduction of the load-carrying
231 capacity of the stabilized layer and load transfer capacity across the cracks, and most
232 importantly cause reflection cracks (Adaska and Luhr 2004). The latter cracks occur in the
233 surface asphaltic course and contribute to a gradual deterioration of the pavement structure.
234 Logically, the rate of such deterioration is largely governed by the rate of which the main
235 structural layer (CBGM layer in this case) deteriorates. Thus, studying how incorporation of
236 fibers might affect the cracking process in the main structural layer (stabilized base course) is
237 an important issue that needs to be clarified in order to understand the damage process and
238 failure mechanism. In addition, this will contribute to explaining and understanding the
239 relationship between cracking features at the meso-scale level and macro-scale properties.

240

241 In concrete, which is a different cementitious material, some researchers have studied,
242 quantitatively, the cracking patterns of fiber-reinforced mixtures and attempted to relate them
243 to mechanical properties. For example, Stang et al. (1990) and Yan et al. (2002) studied the
244 cracking patterns of concrete mixtures reinforced with different types of fiber. Their

245 conclusions indicated that a relationship existed between cracking pattern and mechanical
246 properties. To understand the failure sequence of different types of composites, others (Curbach
247 and Eibl 1990, Pyo et al. 2016) have attempted to monitor the formation of cracks in concrete
248 specimens during load application as a time-dependent process by evaluating the crack
249 propagation speed.

250

251 This paper represents the **first attempt** to investigate the time-dependent fracture of fiber-
252 reinforced and cement-stabilized aggregate mixtures intended to be used as a base layer within
253 a semi-rigid pavement. This was conducted in terms of crack propagation speed and crack
254 diffusion rate. Both of these parameters were characterized, quantitatively, by monitoring the
255 propagation of damage during load application. As is well known, the failure of a pavement
256 structure is a time-dependent process; therefore, the idea of this part of the study was also to
257 investigate how stabilizer (cement) affects the damage process of FCBGMs and to compare this
258 with CBGM behavior, which will eventually lead to understanding of the feasibility of fiber
259 reinforcement in a pavement structure. Such studies, as reported by Stang et al. (1990) and Silva
260 et al. (2009), may also provide essential information to develop models to help simulate the
261 cracking process of such materials.

262

263 **4.1 Crack propagation speed**

264 To monitor the development of the cracks during tensile loading, the non-contact DIC technique
265 described earlier was used to capture videos at a rate of 1000 fps. These videos were used to
266 obtain images (at selected stages of loading) which were then used to estimate the crack lengths.
267 Figure 8 shows samples of captured images at various loading stages for some of the
268 investigated mixtures. Crack propagation speeds were calculated by averaging the crack length-
269 time curves as adopted by Pyo et al. (2016). To estimate the crack lengths, the latter authors
270 used the Canny edge detector algorithm to extract a map of the cracks. In this paper, however,
271 another approach is suggested and has been implemented to calculate the crack lengths. This is

272 due to the nature of the speckled testing surface that makes both cracks and dots appear the
273 same in the image after binarization. Such appearance in the testing surface makes it impossible
274 to extract the cracking patterns using the available thresholding algorithms (Figure 9 a, b). In
275 the suggested methodology, the captured images were inserted into a CAD system, then these
276 images were scaled up to make a meaningful comparison. After that, these cracks were digitized
277 (Figure 9c) using software facilities. Total crack lengths were measured through the CAD
278 software tools. To reduce the processing time, these images were selected at equal time
279 intervals, which depended on the testing time of the specimens. Figure 10 illustrates samples of
280 estimated crack length-time relationships which were used to calculate the crack propagation
281 speed of the investigated mixtures.

282

283 A summary of crack propagation speeds for different mixtures is presented in Figure 11. As is
284 clear from this figure, the addition of more cement to CBGMs accelerates the propagation speed
285 of cracks which might indicate that the rate of deterioration is higher in the case of stiff materials
286 and also ductility decreases because the cracks propagate rapidly before showing further
287 deformation. Using steel fiber reinforcement, in general, reduces the crack propagation speed
288 as shown in the previous figure. This is because the presence of fibers arrests and bridges the
289 cracks and hence reduces their propagation speed. This finding is consistent with outcomes of
290 the studies conducted by Mindess (1995) and Pyo et al. (2016) which confirmed a reduction in
291 the crack speed due to fiber inclusion.

292

293 Another interesting new finding is the clarification of the role that cement content plays in crack
294 propagation speed. Figure 11 indicates that incorporation of higher cement content in the case
295 of FCBGMs is found to decelerate the propagation of the cracks significantly compared to
296 mixtures with low cement content. Crack speed decreased 3.6, 7.6 and 14 times due to
297 incorporation of 0.5% steel fiber at 3%, 5% and 7% cement content, respectively. This can be
298 attributed to the higher bond level between the fiber and the adjacent materials that

299 accompanied the higher cement content which enables these fibers to be more effective in crack
300 arresting-bridging and hence reduces the speed of crack propagation.

301

302 **4.2 Rate of damage (diffusion of cracks)**

303 In addition to the crack propagation speed, another important parameter that affects
304 performance of a stabilized layer is the diffusion rate (or the degree of dispersion) of the cracks
305 inside the body of the cemented layer. The idea of this part of the study was to evaluate diffusion
306 rate (i.e., the rate of damage) as a time-dependent process. This will be achieved through
307 implementation of the fractal geometry concept conducted in terms of fractal dimension by
308 monitoring the evolution of fractal dimension during the load application. Another objective is
309 to estimate the fractal dimension at the end of the test to evaluate the amount of damage that
310 has occurred. Higher fractal dimension indicates, generally, more disordered cracks, which
311 means higher damage (Carpinteri and Yang 1996). Less cracks diffusion or localization of
312 cracks is expected to accelerate the formation of reflection cracks whereas more diffused cracks
313 may help to reduce the potential reflectivity of cracks due to reduced stress concentrations.
314 Logically, fractal dimension should increase with the load application process which means that
315 the damage increases as load increases. However, an interesting question in this regard is: to
316 what extent the fiber might affect the damage rate and the final damage of the cemented
317 aggregate and what is the role that the amount of cement might play in this process.

318

319 To answer this question, the evolution of fractal dimension was estimated during the load
320 application stages for both FCBGMs of different cement content and these were compared with
321 the matching unreinforced mixtures. The following methodology was suggested and
322 implemented: as was conducted in the previous part (Section 4.1), the cracks were extracted at
323 each stage of load application. Next, the fractal dimension was determined using the box-
324 counting method (Chiaia et al. 1998, Hassan 2012, Erdem and Blankson 2013). Then, the fractal
325 dimension-time relationship was constructed and the slope of this curve was computed as the

326 damage evolution rate of the mixture. Figure 12 shows samples of the estimated fractal
327 dimension-time relationships.

328

329 A summary of the damage rate results is illustrated in Figure 13. It can be observed from this
330 figure that, for CBGMs, the rate of fractal dimension propagation (i.e., the rate of damage)
331 increases for the stiffer mixtures as compared with less stiff materials. The rate of damage for
332 FCBGMs, on the other hand, decreases as a consequence of the fiber incorporation at all cement
333 contents. Interestingly, there was a greater reduction in the rate of damage when the fiber-
334 reinforced mixtures were heavily cemented. The rate of damage decreased by a factor of 4, 4.4
335 and 14.6 times upon the addition of 0.5% fiber reinforcement at 3%, 5% and 7% cement
336 contents, respectively.

337

338 These findings, in fact, also reveal the mechanism behind the toughening process of fiber-
339 reinforced mixtures. As can be seen from Figure 14, the reduction in damage correlates well
340 with toughness improvement. In other words, the mixtures of higher toughness have normally
341 had less damage rate (and, of course, lower crack speed) which means that these mixtures are
342 able to carry the additional load after their peak because they are relatively intact and the fibers
343 carry the greatest part of the tensile loads.

344

345 To evaluate the possible mitigation of reflection cracking due to the reduction of crack
346 localization in the FCBGM layer, the fractal dimensions were calculated at the end of testing
347 as stated earlier. Figure 15 illustrates the fractal dimensions for the different mixtures. The
348 general trend is an improvement in the fractal dimension values due to fiber reinforcement
349 which confirms greater crack diffusion inside unreinforced CBGMs. Although this
350 improvement is only about 9%, using higher fiber content will ensure higher dispersion of
351 damage. Furthermore, in combination with the bridging effect this may reduce the reflectivity
352 of the cracks significantly. In their study, Yan et al. (2002) reported that the tensile strength of

353 fiber reinforced concrete, measured through the flexural test, increased proportionally as fractal
354 dimension increased. The fractal dimensions in this paper are also found to have some
355 relationship with the indirect tensile strength as shown in Figure 16.

356

357 **5 Horizontal strain rate**

358 Figure 17 shows a sample of the horizontal tensile strains developed during the application of
359 vertical diametrical compression (applied at a rate of 0.5 mm/min.). The slopes of these average
360 straight lines are considered as the rate of applied horizontal strain. Figure 18 illustrates a
361 summary of these horizontal strain rates. The latter figure indicates that the horizontal strain
362 rate increases with the addition of more cement to the CBGMs while in FCBGMs, an inverse
363 trend can be noticed. The highest reduction in developed horizontal strain occurred at high
364 cement levels, where inclusion of 0.5% fiber-reinforcement in the highly cemented mixture
365 reduced the strain rate 20 times compared to 3 times at low cement content. Most of the
366 developed tensile stresses are, in fact, absorbed by the fibers at both micro and macro scale
367 levels since all cementitious materials are weak in tension. So, when the micro-crack first
368 develops, all tensile stresses are taken by the fibers. Therefore, in this process, the presence of
369 cement plays an important role since it will increase the bond strength of the fiber which in turn
370 increases the tensile resistance.

371

372 Apart from the testing configuration, many researchers have found a relationship between the
373 rate of strain and crack propagation speed. For example, a logarithmic relationship was reported
374 in Pyo et al. (2016)'s study. John and Shah (1986) and Curbach and Eibl (1990) found that the
375 logarithm of strain rate is related linearly with the logarithm of crack speed. In this paper, a
376 logarithmic relationship was also found (Figure 19). This suggests that regardless of the nature
377 of the cement-stabilized aggregate (i.e., the degree of binding and gradation of different
378 cementitious materials), these mixtures behave in a similar way to that observed in concrete

379 mixtures. The rate of damage seems also to be affected by the rate of strain and a logarithmic
380 relationship is also found, as illustrated in the Figure 19.

381

382 Comparing and contrasting crack speeds (at each strain level) of both CBGMs and FCBGMs
383 with those for plain and fiber-reinforced concrete mixtures (Zhang et al. 2015, Pyo et al. 2016)
384 reveals that the cracking speed of the former mixtures is always less (for the same loading rates)
385 than those of the latter concrete mixtures, as shown in Figure 20. This is, logically, attributable
386 to the greater amount of cement that the concrete mixtures have, compared with those used in
387 cement-stabilized aggregates. This might suggest that, from the crack propagation speed point
388 of view, the use of cement-stabilized aggregate mixtures as reinforced layers within a pavement
389 structure is better than that of fiber-reinforced concrete.

390

391 **6 Conclusions**

392 In order to optimize and exploit all recycled steel fiber properties, this paper has examined the
393 effect of cement content on the behavior of fiber reinforced cement-bound aggregate mixtures
394 and unreinforced mixtures as well. To understand this behavior, both macro-scale mechanical
395 properties and time-dependent damage at a meso-scale level have been investigated
396 interactively and in a synergistic way. Based on the findings of this study, the following main
397 conclusions can be stated:

398

399 1. Using more cement generally improves the tensile strength of both reinforced and
400 unreinforced cement-stabilized mixtures. Significant improvement was obtained at higher
401 cement contents when including steel reinforcement. Therefore, to ensure longer pavement
402 life and/or less pavement thickness, it would be sensible to consider use of fiber at higher
403 cement contents.

404

405 2. Regarding the increase in toughness for the investigated mixtures (CBGMs and FCBGMs),
406 a significant improvement occurred with highly cemented mixtures. Nevertheless, the

407 toughness increased after fiber inclusion at all cement contents. Also, cemented mixtures
408 become more ductile after fiber reinforcement and this improvement is more obvious with
409 5% or more cement inclusion. The toughness of fiber-reinforced mixtures comes from a
410 lower damage propagation rate (i.e., lower diffusion rate of cracks inside FCBGMs) which
411 keeps them intact for a relatively long period compared to CBGMs.

412
413

414 3. Using of a greater cement content led to a higher crack propagation speed in the case of
415 mixtures containing no fibers. This means there will be more pavement deterioration after
416 reaching the peak strength of the materials which, in turn, would necessitate maintenance
417 operations that may be expensive or unavailable. On the other hand, use of steel fibers
418 (extracted from waste tires) in cemented mixtures reduces the crack propagation speed at
419 all cement contents with the greatest reduction occurring at high cement contents. This
420 would suggest only a gradual deterioration of the FCBGM until the pavement reaches its
421 ultimate capacity and, even after this stage, would probably result in a lengthy period before
422 maintenance application is needed.

423
424

425 4. The rate of crack diffusion increases as cement content of the CBGMs increases which
426 means that a highly cemented pavement layer will deteriorate more rapidly compared with
427 mixtures containing less cement. With high cement content, if necessary, the use of fiber
428 will contribute to delaying the rate of crack diffusion and hence ensure longer pavement
429 life. Unlike lightly stabilized CBGMs, increasing the amount of cement in FCBGMs
effectively decreases the rate of damage propagation.

430
431

432 5. In the light of the benefits obtained from fiber incorporation at high cement content, it is
433 recommended that this reinforcement should be used with a cement content not less than
5%.

434
435

436 By combining these results, it can be concluded that incorporation of recycled steel fiber
437 reinforcement at high cement content is most beneficial in CBGMs since this will result in
438 significant improvement of indirect tensile strength. In addition, it will delay the crack
439 propagation speed and crack diffusion rate. The implications of these findings are a reduction
440 in the required thickness of the stabilized layer and a delay in pavement failure. In addition, this
441 reinforcement will also reduce the decay of the pavement after reaching its service life, which
442 will provide more time before maintenance is required – important in cases of limited funds for
443 such pavement projects.

444

445

446

447 **Acknowledgements**

448 The authors would like to acknowledge the support of the University of Nottingham.
449 Appreciation is also extended to Mr. Jason Greaves, Mr. Tom Buss, Mr. Nigel Rook and Mr.
450 Richard Blackmore for helping in the experimental program.

451

452

453

454

455

456

457

458 **Figure Captions**

459 Figure 1: Gradation of aggregate.

460 Figure 2: Appearance of the steel fibres extracted from old vehicle tires.

461 Figure 3: Sample preparation (a); Testing setup (b) and close-up view (c) of indirect tensile
462 testing.

463 Figure 4: Effect of fiber reinforcement on ITS values.

464 Figure 5: Stress-strain curves for different fiber and cement levels: a. C3F0; b.C3F0.5; c. C5F0;
465 d.C5F0.5; e. C7F0 and C7F0.5

466 Figure 6: Absolute toughness for different of fiber and cement contents.

467 Figure 7: Deformability properties for various investigated mixtures.

468 Figure 8: Selected crack propagation stages for some of the investigated mixtures: a. C3F0; b.
469 C3F0.5; c. C7F0 and d. C7F0.5

470 Figure 9: Extracting cracking patterns: a. cracked section; b. image binarization; c. digitization
471 of the cracks and d. extracted cracks.

472 Figure 10: Samples of crack length propagation versus time used to estimate crack propagation
473 speeds.

474 Figure 11: Summary of crack propagation speeds for CBGMs and FCBGMs.

475 Figure 12: Samples of fractal dimensions against time, used to estimate fractal dimension
476 propagation rate.

477 Figure 13: Summary of damage propagation rate expressed as fractal dimension evolution rate.

478 Figure 14: Toughness- damage rate relationship.

479 Figure 15: Terminal fractal dimensions for investigated mixtures.

480 Figure 16: ITS-Fractal dimension relationship.

481 Figure 17: Samples of horizontal tensile strain development during the application of vertical
482 compressive displacement at constant rate.

483 Figure 18: Summary of developed horizontal tensile strains at different cement contents.

484 Figure 19: Relationship of cracking speed and damage rate with horizontal tensile strain.

485 Figure 20: Comparison with previous crack speed-strain rate relationships obtained for different
486 types of concrete mixture.

487

488

489

490

Table 1: Mix designation, proportions and densities of different components

491

492

493

494

495

496

497

498

499

500

501

Mixture ID	cement content ¹ ,%	Fibers content ² ,%	Water content ³ ,%	Density, kg/m ³
C3F0	3	0	4.5	2534.90 (4.4)*
C5F0	5	0	4.6	2532.24 (2.2)
C7F0	7	0	4.7	2528.90 (3.9)
C3F0.5	3	0.5	4.5	2517.51 (6.6)
C5F0.5	5	0.5	4.6	2539.70 (2.1)
C7F0.5	7	0.5	4.7	2539.95 (7.3)

502

¹ by the weight of dry aggregate (and fibers for reinforced mixes).

503

² by the weight of dry aggregate.

504

³ by the weight of dry aggregate, (fiber for reinforced mixes) and cement.

505

*the numbers in the bracket are standard error of the mean

506

507

508

509

Figure 1: Gradation of aggregate.

510

511

512

513

514

515

516

517

518

519

520

521

522

523

524

525

526

527

528

529

530

531

532

533

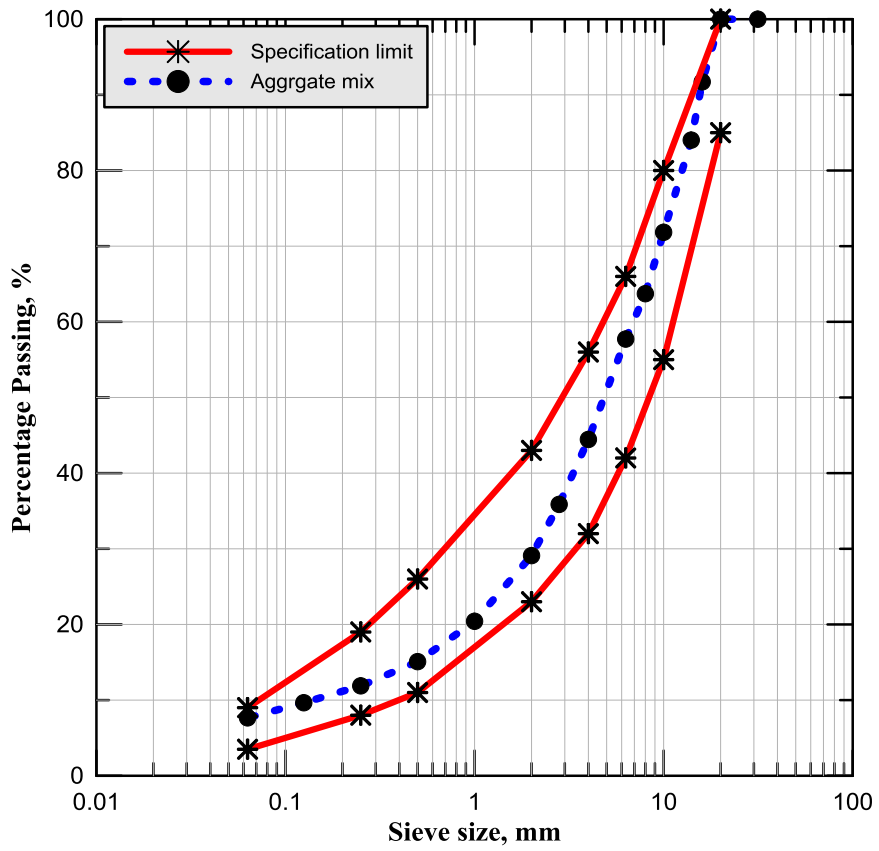
534

535

536

537

538



539 Figure 2: Appearance of the steel fibres extracted from old vehicle tires.

540

541

542

543

544

545

546

547

548

549

550



551

552

553

554

555

556

557

558

559

560

561

562

563

564

565

566

567

568

569 Figure 3: Sample preparation (a); Testing setup (b) and close-up view (c) of indirect tensile testing

570

571

572

573

574

575

576

577

578



579

580

581

582

583

584

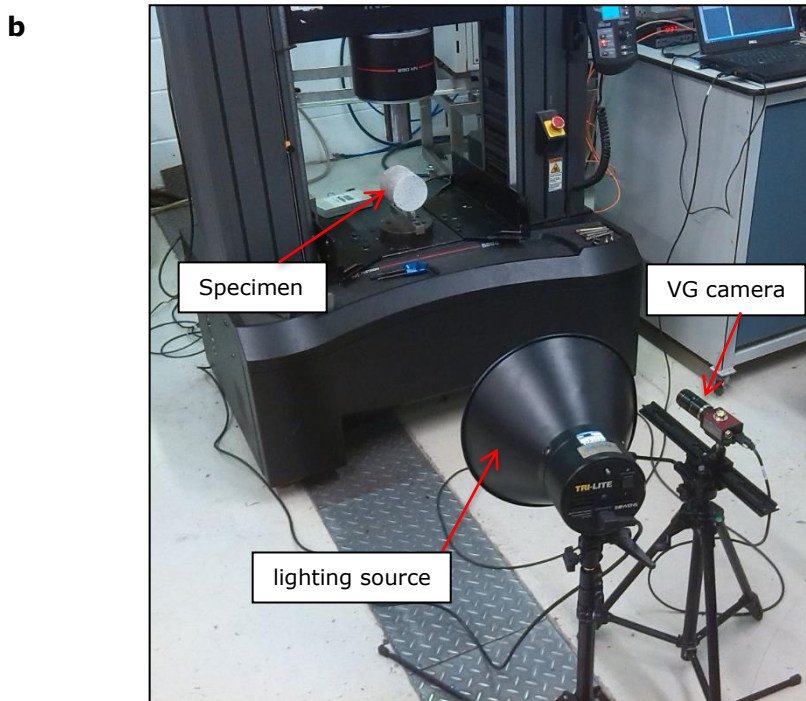
585

586

587

588

589



590

591

592

593

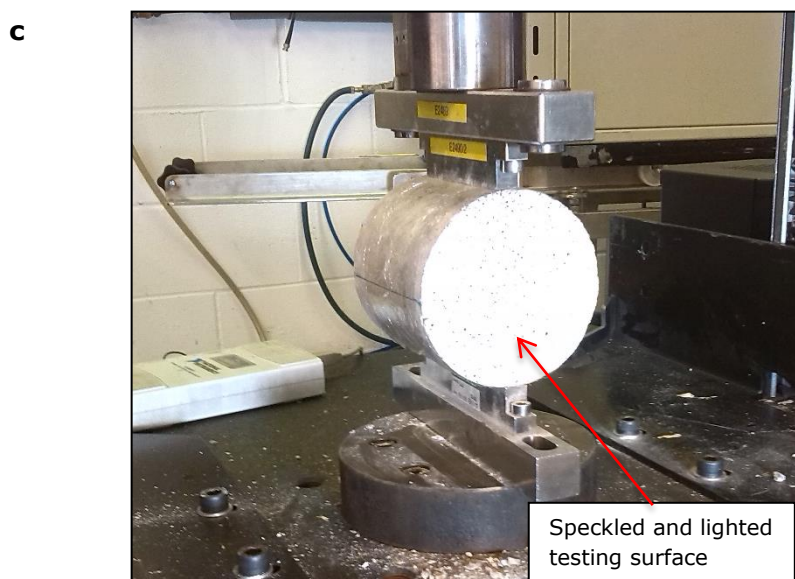
594

595

596

597

598



599

Figure 4: Effect of fiber reinforcement on ITS values.

600

601

602

603

604

605

606

607

608

609

610

611

612

613

614

615

616

617

618

619

620

621

622

623

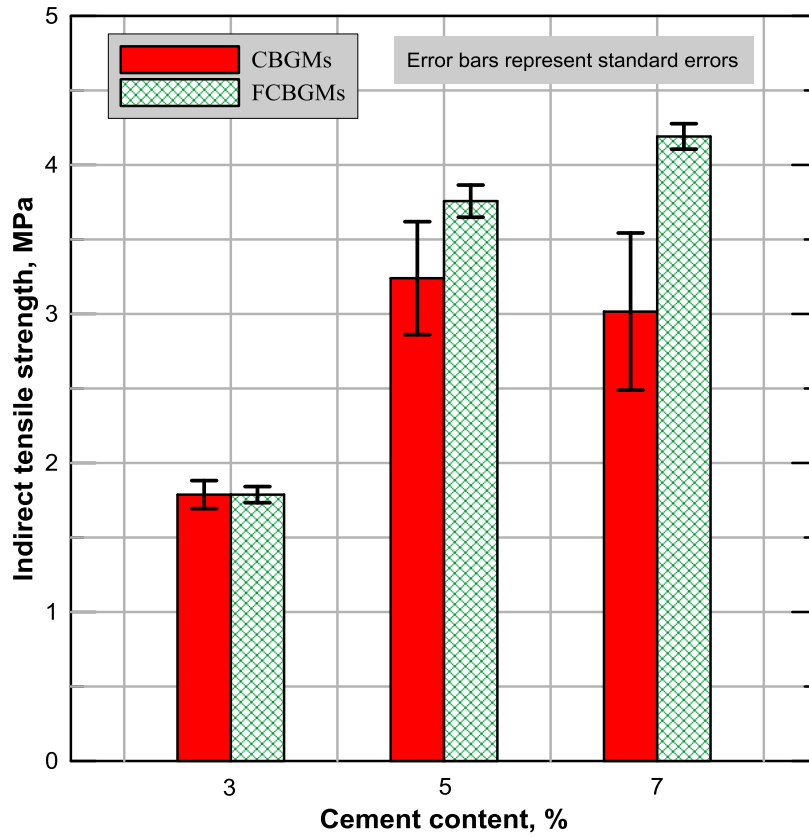
624

625

626

627

628



629

Figure 5: Stress-strain curves for different fiber and cement levels: a. C3F0; b.C3F0.5; c. C5F0;

630

d.C5F0.5; e. C7F0 and C7F0.5

631

634

635

636

638

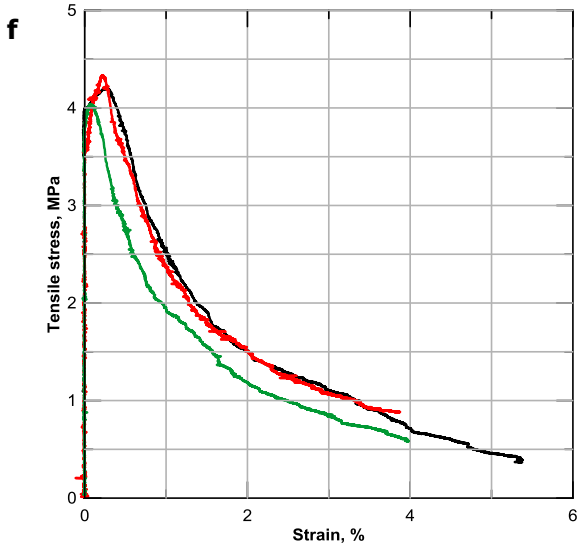
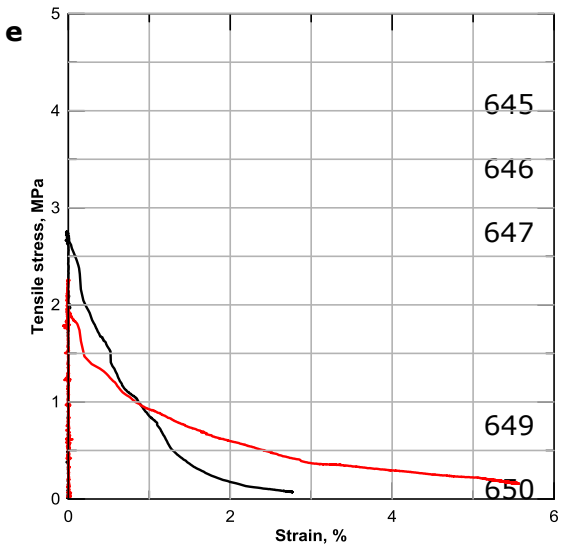
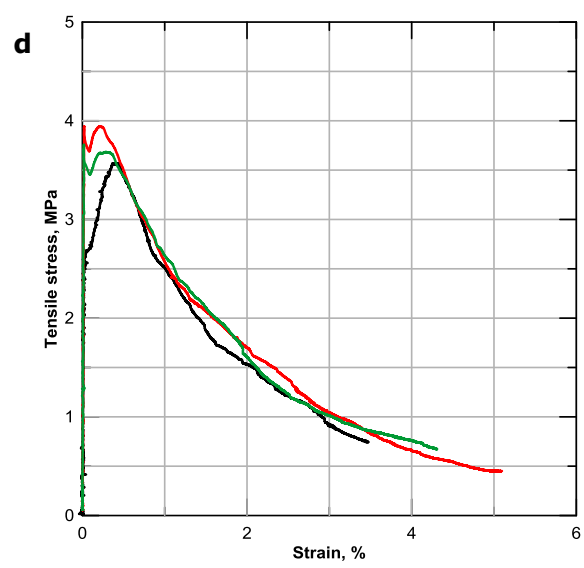
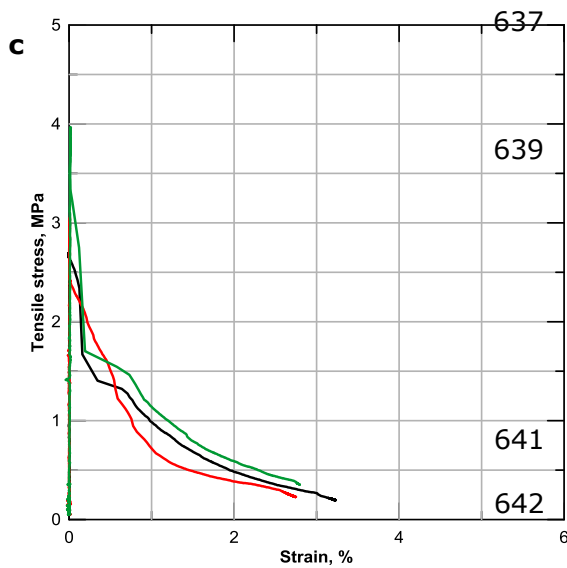
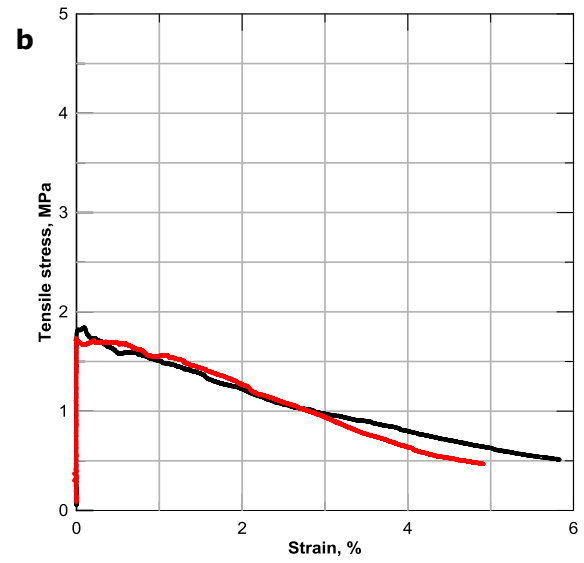
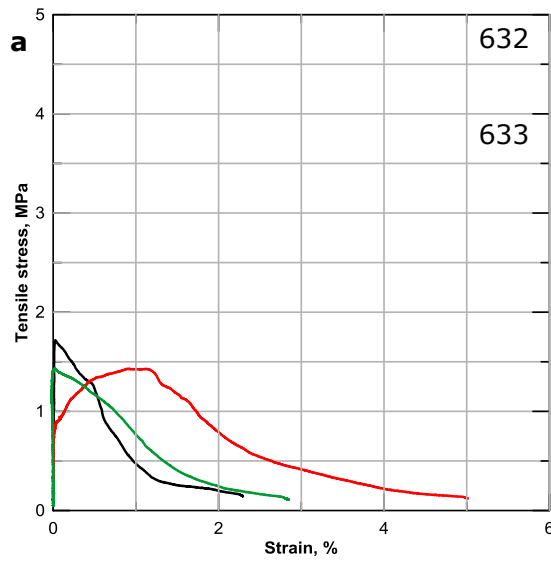
640

643

644

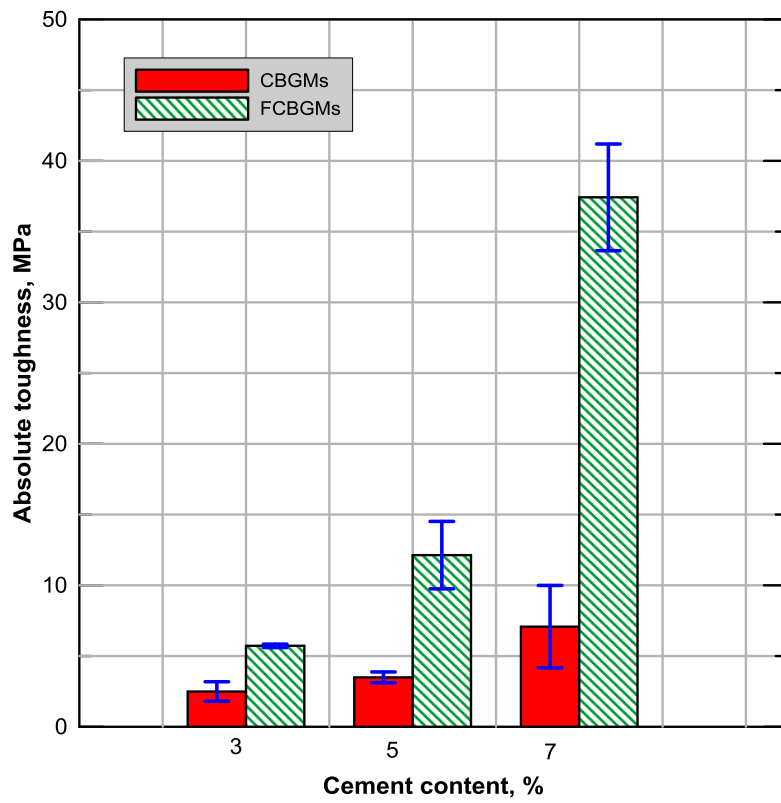
648

651



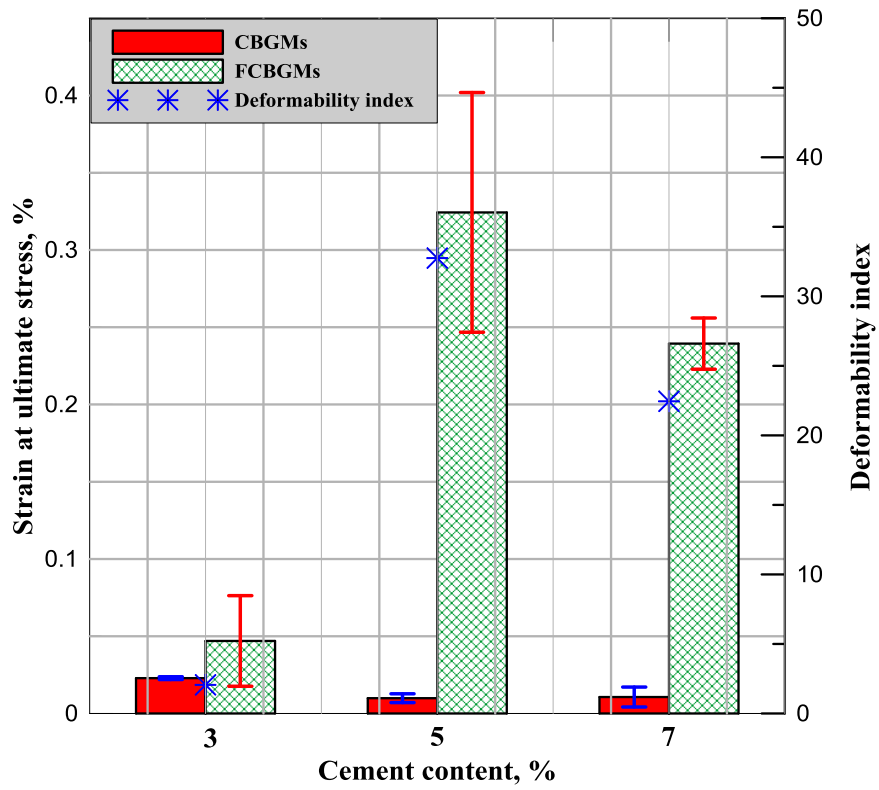
652
653
654
655
656
657
658
659
660
661
662
663
664
665
666
667
668
669
670
671
672
673
674
675
676
677
678
679

Figure 6: Absolute toughness for different of fiber and cement contents.



680
681
682
683
684
685
686
687
688
689
690
691
692
693
694
695
696
697
698
699
700
701
702
703
704
705
706
707

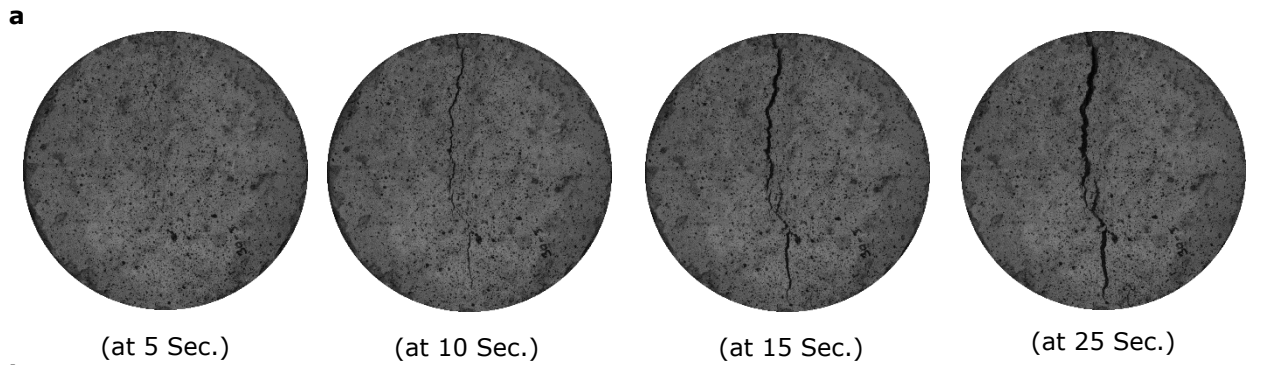
Figure 7: Deformability properties for various investigated mixtures.



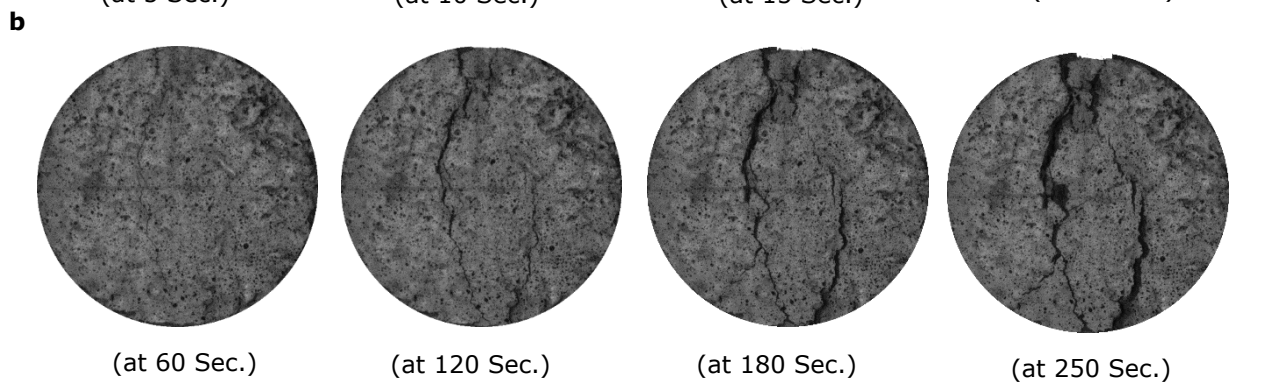
708 Figure 8: Selected crack propagation stages for some of the investigated mixtures: a. C3F0; b.
709 C3F0.5; c. C7F0 and d. C7F0.5

710

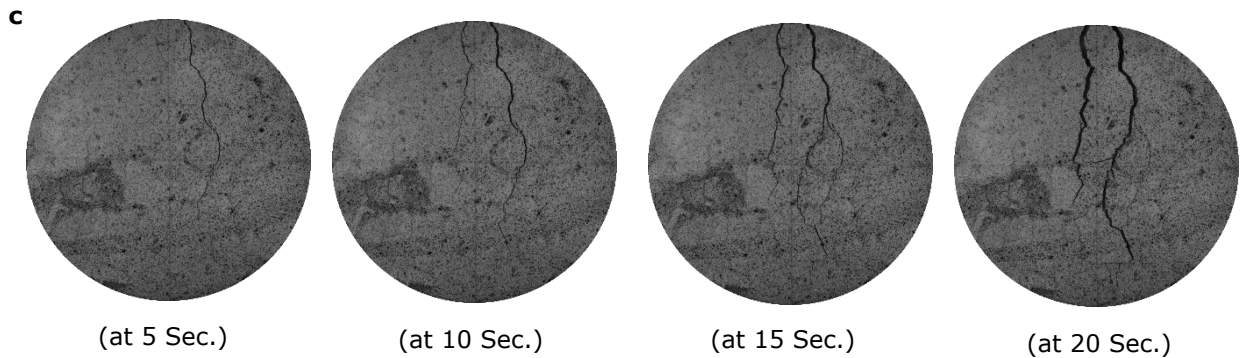
711



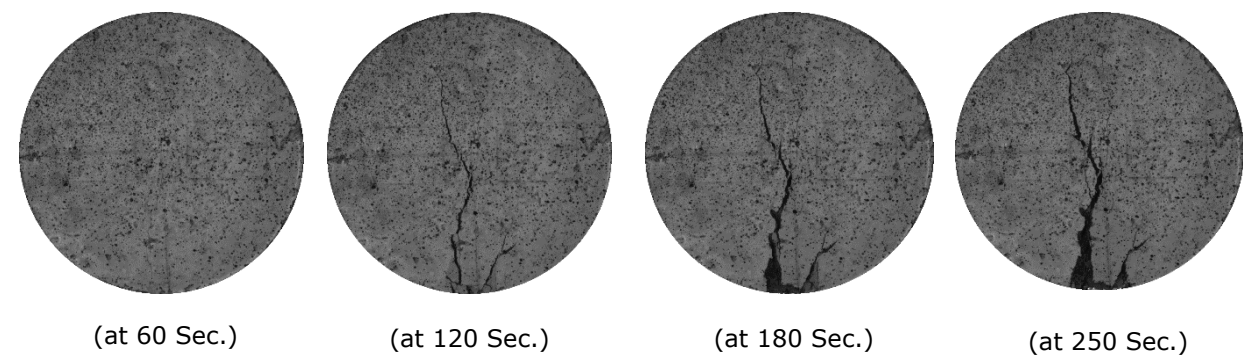
717



724



730



737

738 Figure 9: Extracting cracking patterns: a. cracked section; b. image binarization;
739 of the cracks and d. extracted cracks

740

741

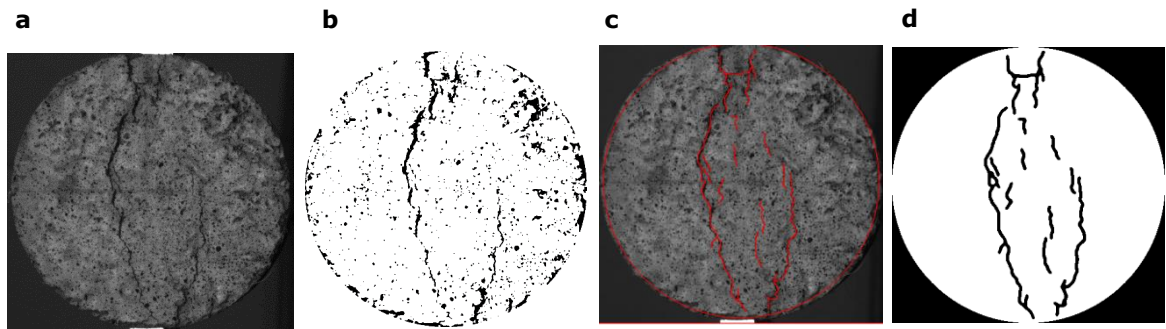
742

743

744

745

746



747

748

749

750

751

752

753

754

755

756

757

758

759

760

761

762

763

764

765

766

767

768 Figure 10: Samples of crack length propagation versus time used to estimate crack propagation

769

770

771

772

773

774

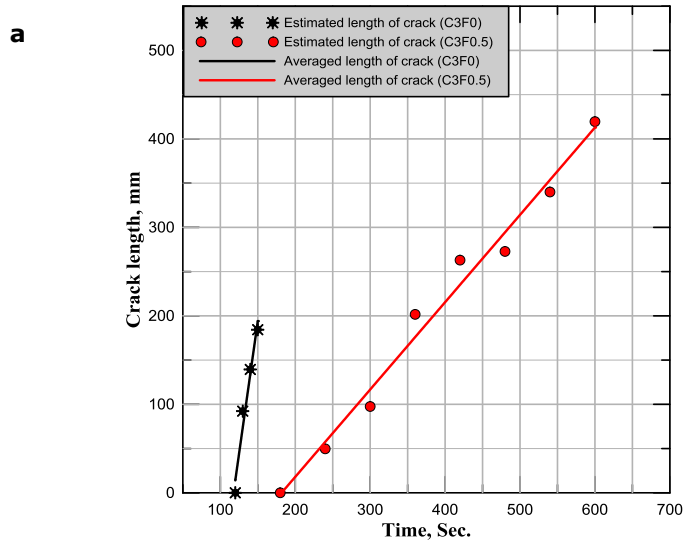
775

776

777

778

779



780

781

782

783

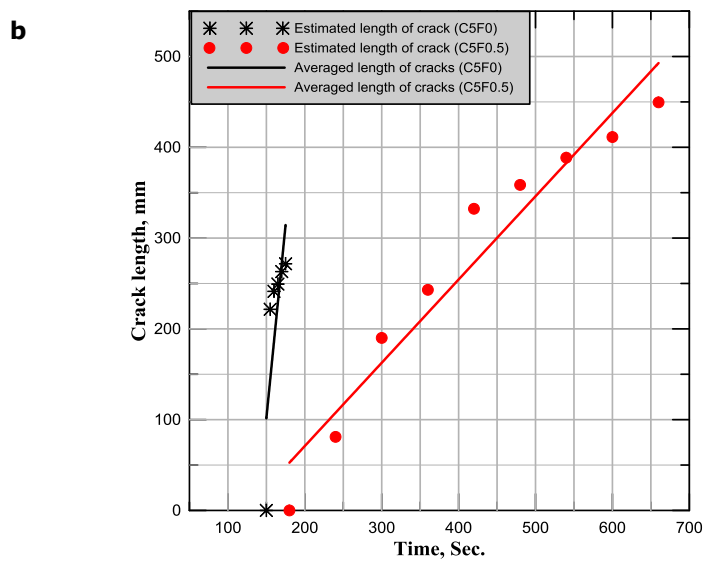
784

785

786

787

788



789

790

791

792

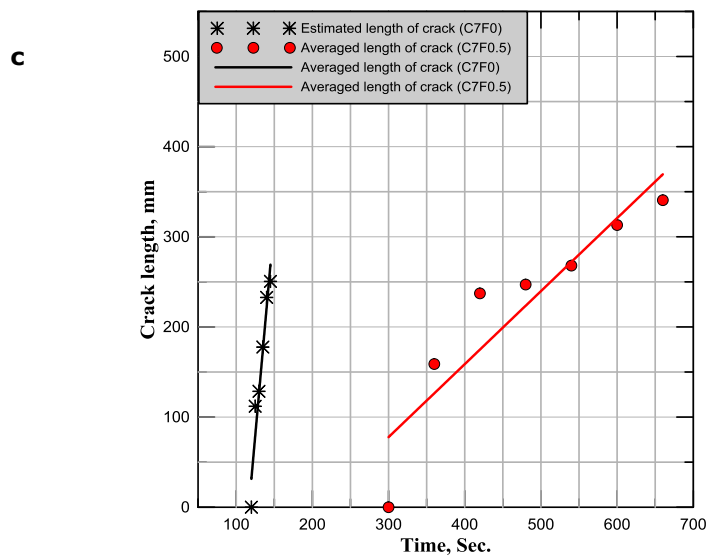
793

794

795

796

797



798
799
800
801
802
803
804
805
806
807
808
809
810
811
812
813
814
815
816
817
818
819
820
821
822
823
824
825
826
827

Figure 11: Summary of crack propagation speeds for CBGMs and FCBGMs

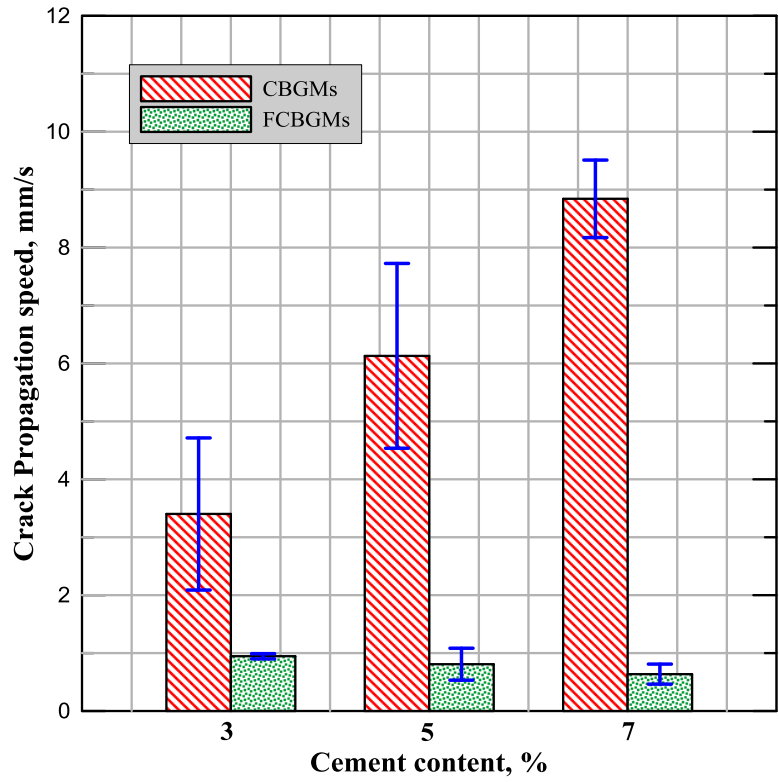
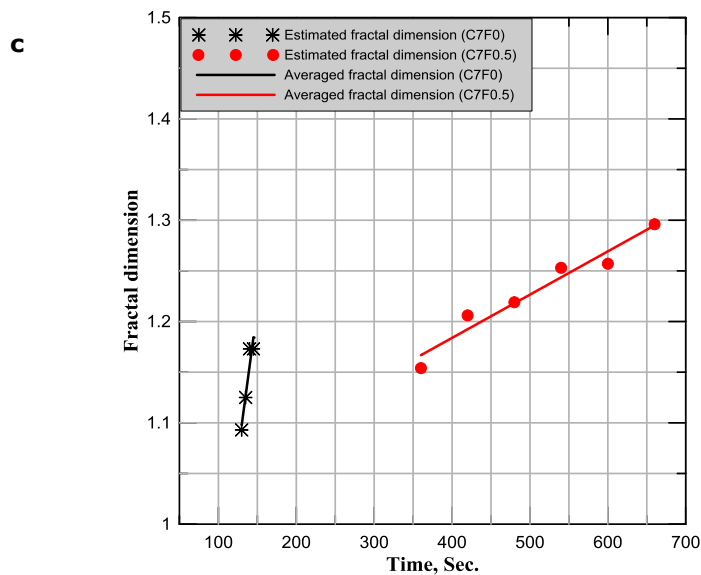
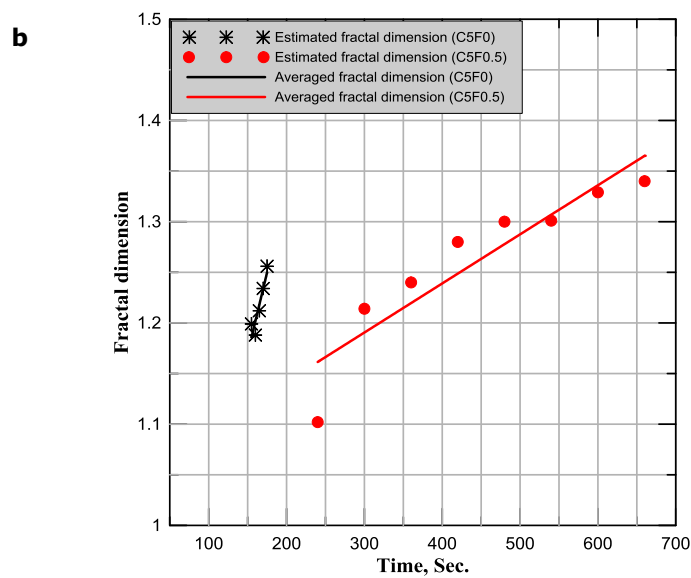
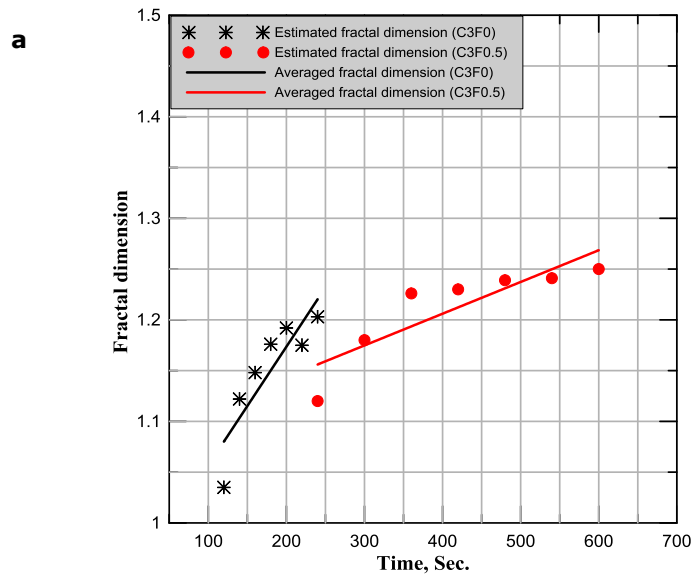


Figure 12: Samples of fractal dimensions against time, used to estimate fractal dimension propagation rate



859 Figure 13: Summary of damage propagation rate expressed as fractal dimension evolution rate

860

861

862

863

864

865

866

867

868

869

870

871

872

873

874

875

876

877

878

879

880

881

882

883

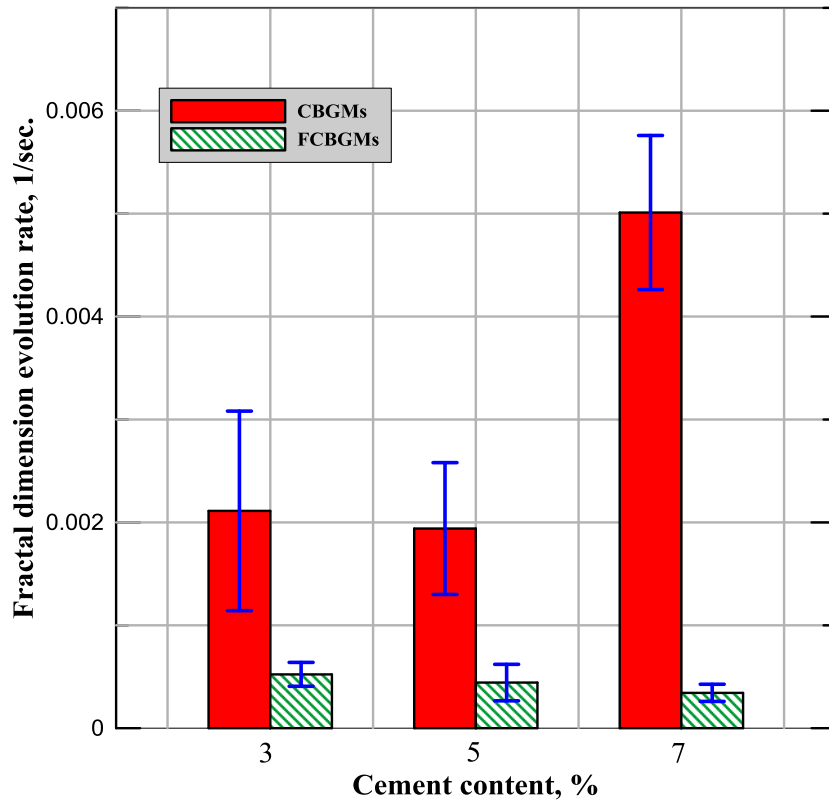
884

885

886

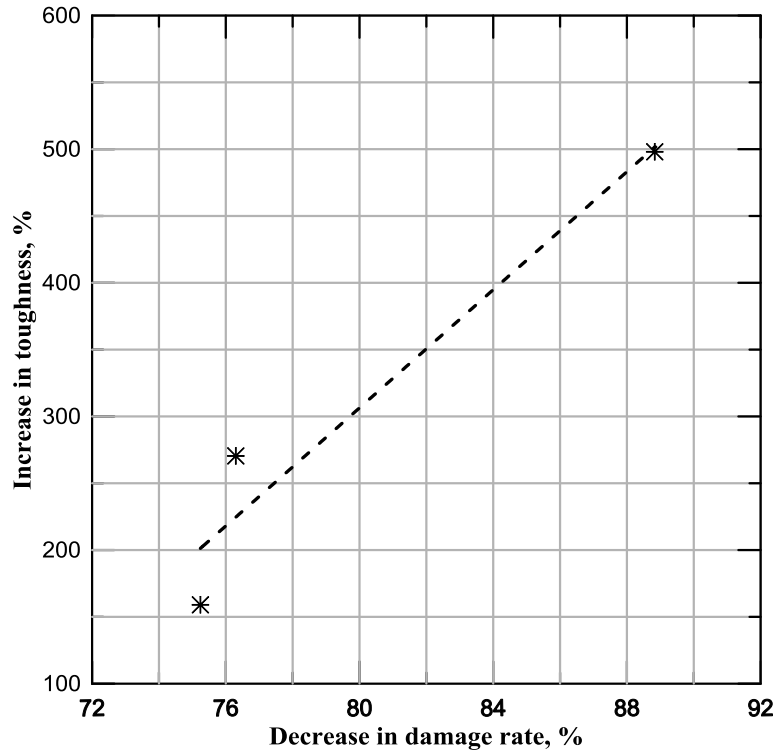
887

888



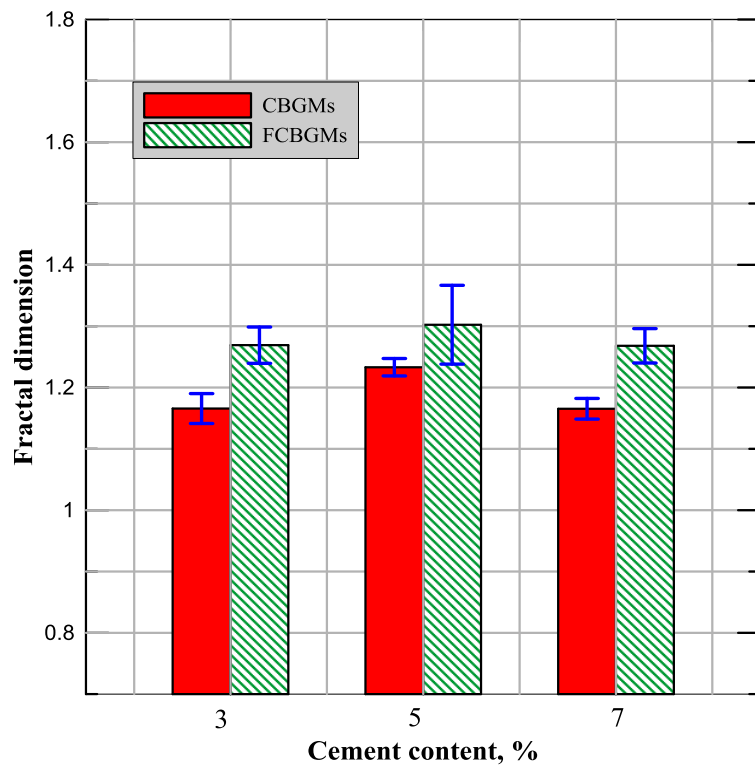
889
890
891
892
893
894
895
896
897
898
899
900
901
902
903
904
905
906
907
908
909
910
911
912
913
914
915
916
917
918

Figure 14: Toughness- damage rate relationship.



919
920
921
922
923
924
925
926
927
928
929
930
931
932
933
934
935
936
937
938
939
940
941
942
943
944
945
946
947
948

Figure 15: Terminal fractal dimensions for investigated mixtures.



949 Figure 16: ITS-Fractal dimension relationship.

950

951

952

953

954

955

956

957

958

959

960

961

962

963

964

965

966

967

968

969

970

971

972

973

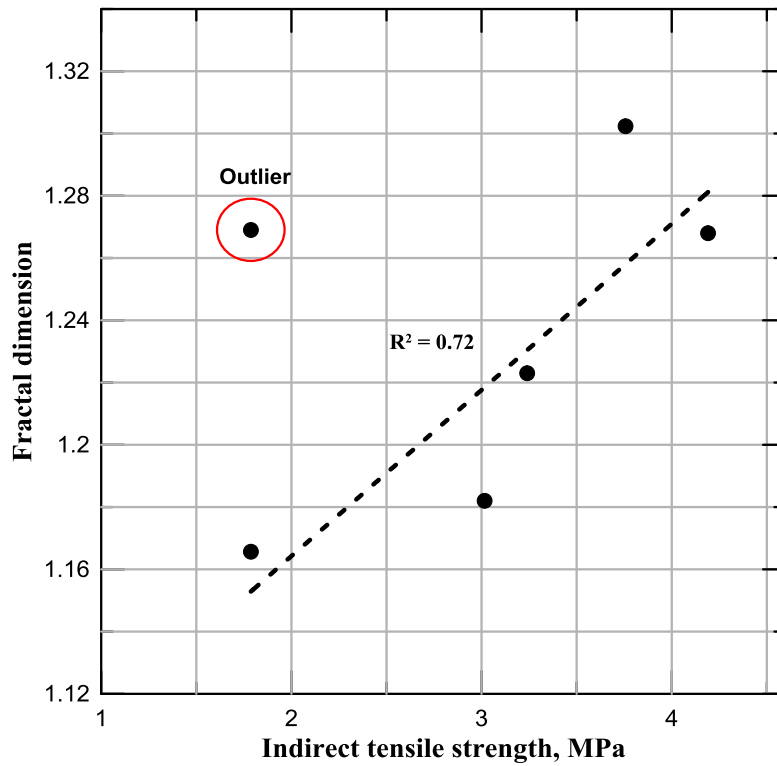
974

975

976

977

978



979 Figure 17: Samples of horizontal tensile strain development during the application of
980 vertical compressive displacement at constant rate

981

982

983

984

985

986

987

988

989

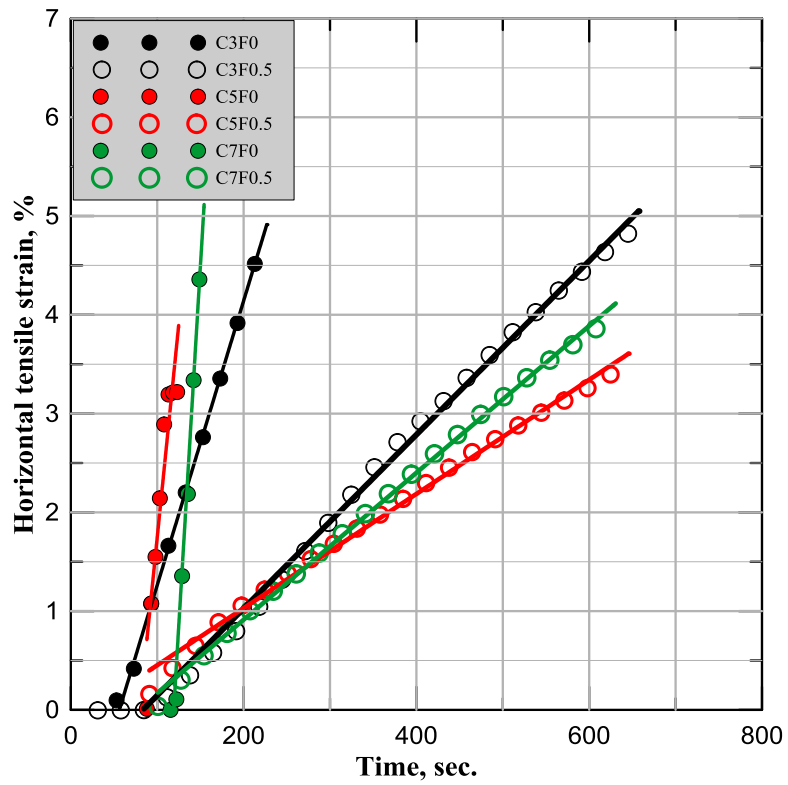
990

991

992

993

994



995

996

997

998

999

1000

1001

1002

1003

1004

1005

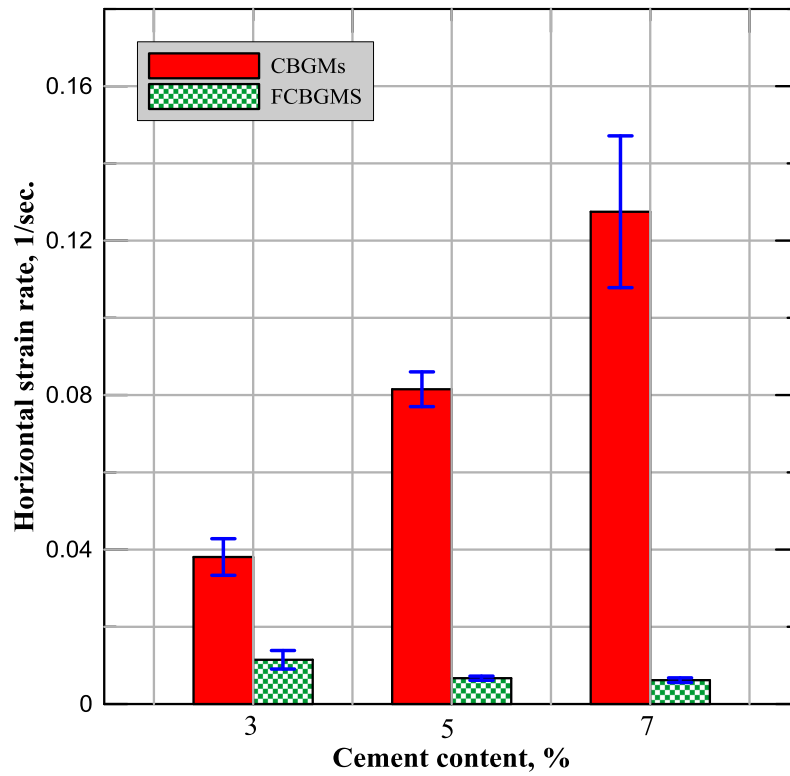
1006

1007

1008

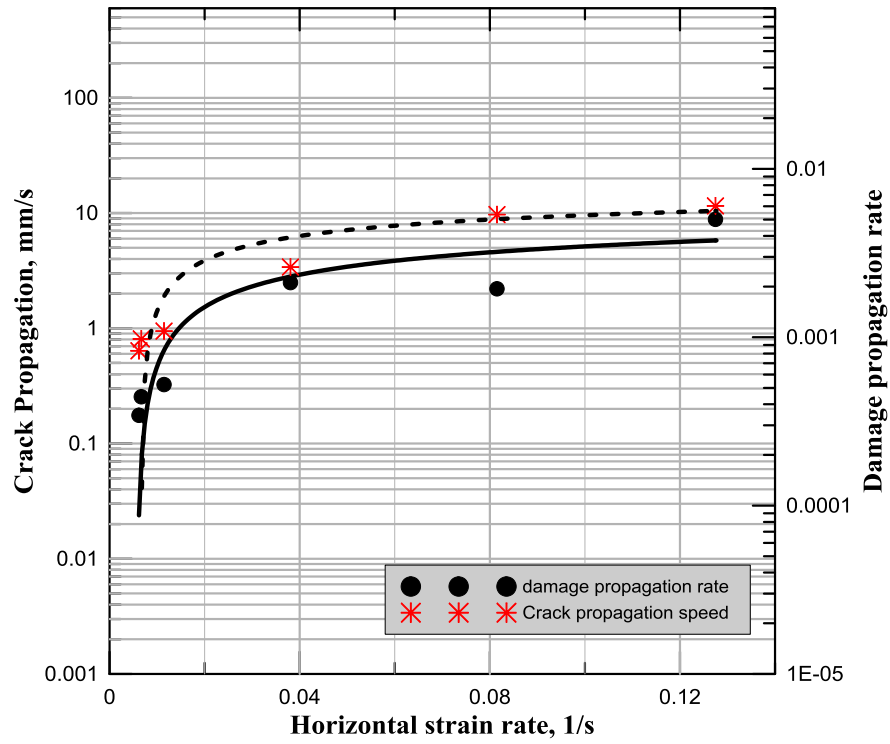
1009
1010
1011
1012
1013
1014
1015
1016
1017
1018
1019
1020
1021
1022
1023
1024
1025
1026
1027
1028
1029
1030
1031
1032
1033
1034
1035
1036
1037
1038

Figure 18: Summary of developed horizontal tensile strains at different cement contents.

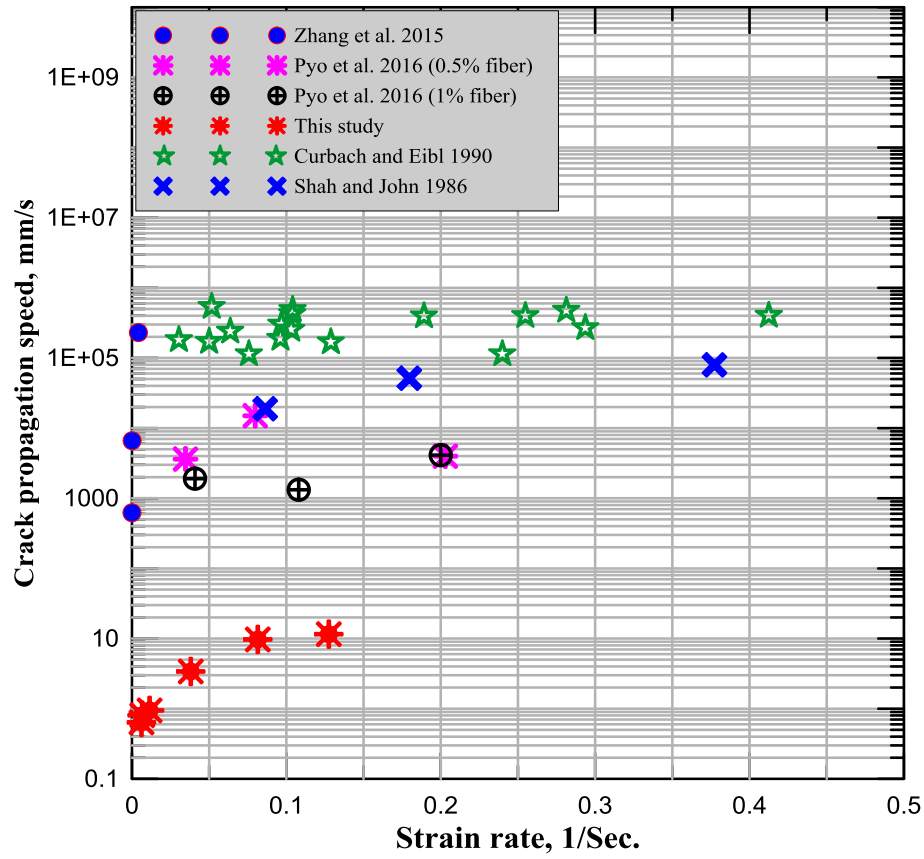


1039
1040
1041
1042
1043
1044
1045
1046
1047
1048
1049
1050
1051
1052
1053
1054
1055
1056
1057
1058
1059
1060
1061
1062
1063
1064
1065
1066
1067
1068

Figure 19: Relationship of cracking speed and damage rate with horizontal tensile strain.



1069 Figure 20: Comparison with previous crack speed-strain rate relationships obtained for
 1070 different types of concrete mixture



1099 **References**

- 1100 Adaska, W. S. and Luhr D. R. (2004). Control of reflective cracking in cement stabilized
1101 pavements. Fifth International RILEM Conference on Reflective Cracking in Pavements,
1102 RILEM Publications SARL.
- 1103 Aiello, M. A., Leuzzi F., Centonze G. and Maffezzoli A. (2009). "Use of steel fibres recovered
1104 from waste tyres as reinforcement in concrete: pull-out behaviour, compressive and
1105 flexural strength." Waste Manag **29**(6): 1960-1970.
- 1106 Angelakopoulos, H., Papastergiou P. and Pilakoutas K. (2015). "Fibrous roller-compacted
1107 concrete with recycled materials – feasibility study." Magazine of Concrete Research
1108 **67**(15): 801-811.
- 1109 Arulrajah, A., Disfani M. M., Haghghi H., Mohammadinia A. and Horpibulsuk S. (2015).
1110 "Modulus of rupture evaluation of cement stabilized recycled glass/recycled concrete
1111 aggregate blends." Construction and Building Materials **84**: 146-155.
- 1112 Arulrajah, A., Mohammadinia A., D'Amico A. and Horpibulsuk S. (2017). "Cement kiln dust
1113 and fly ash blends as an alternative binder for the stabilization of demolition aggregates."
1114 Construction and Building Materials **145**: 218-225.
- 1115 Arulrajah, A., Mohammadinia A., Phummiphan I., Horpibulsuk S. and Samingthong W.
1116 (2016). "Stabilization of Recycled Demolition Aggregates by Geopolymers comprising
1117 Calcium Carbide Residue, Fly Ash and Slag precursors." Construction and Building Materials
1118 **114**: 864-873.
- 1119 Balkis, A. P. (2017). "The effects of waste marble dust and polypropylene fiber contents
1120 on mechanical properties of gypsum stabilized earthen." Construction and Building
1121 Materials **134**: 556-562.
- 1122 British Standards Institution (2013). BS EN 14227-1: Hydraulically Bound Mixtures.
1123 Cement Bound granular Mixtures, The British Standards Institution, London, UK
- 1124
- 1125 Caggiano, A., Xargay H., Folino P. and Martinelli E. (2015). "Experimental and numerical
1126 characterization of the bond behavior of steel fibers recovered from waste tires embedded
1127 in cementitious matrices." Cement and Concrete Composites **62**: 146-155.
- 1128 Carpinteri, A. and Yang G. (1996). "Fractal dimension evolution of microcrack net in
1129 disordered materials." Theoretical and applied fracture mechanics **25**(1): 73-81.
- 1130 Chen, M., Shen S.-L., Arulrajah A., Wu H.-N., Hou D.-W. and Xu Y.-S. (2015). "Laboratory
1131 evaluation on the effectiveness of polypropylene fibers on the strength of fiber-reinforced
1132 and cement-stabilized Shanghai soft clay." Geotextiles and Geomembranes **43**(6): 515-
1133 523.
- 1134 Chiaia, B., Van Mier J. and Vervuurt A. (1998). "Crack growth mechanisms in four different
1135 concretes: microscopic observations and fractal analysis." Cement and Concrete Research
1136 **28**(1): 103-114.
- 1137 Coni, M. and Pani S. (2007). Fatigue analysis of fiber-reinforced cement treated bases. 4th
1138 International SIIV Congress. Palermo (Italy).
- 1139 Cristelo, N., Cunha V. M., Gomes A. T., Araújo N., Miranda T. and de Lurdes Lopes M.
1140 (2017). "Influence of fibre reinforcement on the post-cracking behaviour of a cement-
1141 stabilised sandy-clay subjected to indirect tensile stress." Construction and Building
1142 Materials **138**: 163-173.
- 1143 Curbach, M. and Eibl J. (1990). "Crack velocity in concrete." Engineering Fracture
1144 Mechanics **35**(1-3): 321-326.
- 1145 Erdem, S. and Blankson M. A. (2013). "Fractal–fracture analysis and characterization of
1146 impact-fractured surfaces in different types of concrete using digital image analysis and
1147 3D nanomap laser profilometry." Construction and Building Materials **40**: 70-76.
- 1148 Farhan, A. H., Dawson A. R. and Thom N. H. (2016). "Characterization of rubberized
1149 cement bound aggregate mixtures using indirect tensile testing and fractal analysis."
1150 Construction and Building Materials **105**: 94-102.
- 1151 Farhan, A. H., Dawson A. R. and Thom N. H. (2016). "Effect of cementation level on
1152 performance of rubberized cement-stabilized aggregate mixtures." Materials & Design **97**:
1153 98-107.

1154 Farhan, A. H., Dawson A. R., Thom N. H., Adam S. and Smith M. J. (2015). "Flexural
1155 characteristics of rubberized cement-stabilized crushed aggregate for pavement structure."
1156 Materials & Design **88**: 897-905.

1157 Hassan, N. A. (2012). Microstructural characterization of rubber modified asphalt mixtures
1158 PhD thesis, The university of Nottingham.

1159 John, R. and Shah S. P. (1986). "Fracture of concrete subjected to impact loading."
1160 Cement, concrete and aggregates **8**(1): 24-32.

1161 Kim, S. B., Yi N. H., Kim H. Y., Kim J.-H. J. and Song Y.-C. (2010). "Material and structural
1162 performance evaluation of recycled PET fiber reinforced concrete." Cement and Concrete
1163 Composites **32**(3): 232-240.

1164 Li, Y., Sun X. and Yin J. (2010). Mix design of cement-stabilized recycled aggregate base
1165 course material. Paving Materials and Pavement Analysis: 184-192.

1166 Mindess, S. (1995). "Crack velocities in concrete subjected to impact loading." Canadian
1167 Journal of Physics **73**: 310-314.

1168 Mirzababaei, M., Miraftab M., Mohamed M. and McMahon P. (2012). "Unconfined
1169 compression strength of reinforced clays with carpet waste fibers." Journal of Geotechnical
1170 and Geoenvironmental Engineering **139**(3): 483-493.

1171 Mohammadinia, A., Arulrajah A., Haghghi H. and Horpibulsuk S. (2017). "Effect of lime
1172 stabilization on the mechanical and micro-scale properties of recycled demolition
1173 materials." Sustainable Cities and Society **30**: 58-65.

1174 Mohammadinia, A., Arulrajah A., Horpibulsuk S. and Chinkulkijniwat A. (2017). "Effect of
1175 fly ash on properties of crushed brick and reclaimed asphalt in pavement base/subbase
1176 applications." Journal of Hazardous Materials **321**: 547-556.

1177 Park, S.-S. (2011). "Unconfined compressive strength and ductility of fiber-reinforced
1178 cemented sand." Construction and Building Materials **25**(2): 1134-1138.

1179 Puppala, A. J., Pedarla A., Chittoori B., Ganne V. K. and Nazarian S. (2017). "Long-Term
1180 Durability Studies on Chemically Treated Reclaimed Asphalt Pavement Material as a Base
1181 Layer for Pavements." Transportation Research Record: Journal of the Transportation
1182 Research Board(2657): 1-9.

1183 Pyo, S., Alkaysi M. and El-Tawil S. (2016). "Crack propagation speed in ultra high
1184 performance concrete (UHPC)." Construction and Building Materials **114**: 109-118.

1185 Shahid, M. A. (1997). "Improved Cement Bound Base Design for Flexible Composite
1186 Pavement." PhD Thesis, University of Nottingham.

1187 Silva, F. d. A., Mobasher B. and Filho R. D. T. (2009). "Cracking mechanisms in durable
1188 sisal fiber reinforced cement composites." Cement and Concrete Composites **31**(10): 721-
1189 730.

1190 Sobhan, K. and Mashnad M. (2000). "Fatigue durability of stabilized recycled aggregate
1191 base course containing fly ash and waste-plastic strip reinforcement." Final Rep. Submitted
1192 to the Recycled Materials Resource Centre, Univ. of New Hampshire.

1193 Sobhan, K. and Mashnad M. (2002). "Fatigue damage in roller-compacted pavement
1194 foundation with recycled aggregate and waste plastic strips." Transportation Research
1195 Record: Journal of the Transportation Research Board(1798): 8-16.

1196 Sobhan, K. and Mashnad M. (2003). "Fatigue behavior of a pavement foundation with
1197 recycled aggregate and waste HDPE strips." Journal of geotechnical and geoenvironmental
1198 engineering **129**(7): 630-638.

1199 Stang, H., Mobasher B. and Shah S. P. (1990). "Quantitative damage characterization in
1200 polypropylene fiber reinforced concrete." Cement and Concrete Research **20**(4): 540-558.

1201 Taha, R., Al-Harthy A., Al-Shamsi K. and Al-Zubeidi M. (2002). "Cement stabilization of
1202 reclaimed asphalt pavement aggregate for road bases and subbases." Journal of Materials
1203 in Civil Engineering **14**(3): 239-245.

1204 Thompson, I. (2001). "Use of Steel Fibers to Reinforce Cement Bound Roadbase." PhD
1205 Thesis, University of Nottingham.

1206 Xuan, D., Houben L., Molenaar A. and Shui Z. (2012). "Mixture optimization of cement
1207 treated demolition waste with recycled masonry and concrete." Materials and structures
1208 **45**(1-2): 143-151.

1209 Yan, A., Wu K. and Zhang X. (2002). "A quantitative study on the surface crack pattern of
1210 concrete with high content of steel fiber." Cement and concrete research **32**(9): 1371-
1211 1375.

1212 Zhang, P., Liu C.-h., Li Q.-f. and Zhang T.-h. (2013). "Effect of polypropylene fiber on
1213 fracture properties of cement treated crushed rock." Composites Part B: Engineering **55**:
1214 48-54.
1215 Zhang, X., Ruiz G. and Abd Elazim A. M. (2015). "Loading rate effect on crack velocities in
1216 steel fiber-reinforced concrete." International Journal of Impact Engineering **76**: 60-66.

1217

1218